EUROPEAN MECHANICAL SCIENCE

Research Article

e-ISSN: 2587-1110

Solution scheme development of the nonhomogeneous heat conduction equation in cylindrical coordinates with Neumann boundary conditions by finite difference method

Melih Yıldız[1*]

[1]Iğdır University, Faculty of Engineering, Department of Mechanical Engineering/ Türkiye

Orcid: M. Yıldız (0000-0002-6904-9131)

Abstract: Partial differential heat conduction equations are typically used to determine temperature distribution within any solid domain. The difficulty and complexity of the solution of the equation depend on differential equation characteristics, boundary conditions, coordinate systems, and the number of dependent variables. In the current study, the numerical solution schemes were developed by the Explicit Finite Difference and the Implicit Method- the Crank-Nicolson techniques for the partial differential heat conduction equation including heat generation term described as one-dimensional, time-dependent with the Neumann boundary conditions. The solution schemes were, then, applied to the battery problem including highly varying heat generation. Besides, the solution of the problem was performed by using Matlab pdepe solver to verify the developed schemes. Results suggest that the Crank-Nicolson scheme is unconditionally stable, whereas the explicit scheme is only stable when the Courant-Friedrichs-Lewy condition requirement is less than 0.3404. Comparing the developed schemes to the results obtained from the pdepe solver, the schemes are as reliable as the pdepe solver with certain grid structures. Besides, the developed numerical schemes allow for shorter computational times than the pdepe solver at the same grid structures when considering CPU times.

Keywords: Heat conduction, heat generation, Neumann boundary condition, Crank-Nicolson, pdepe solver.

1. Introduction

Determining the temperature distribution within a solid medium is crucial for various engineering and scientific applications, ranging from the design of efficient heating or cooling systems to predicting material behavior under thermal stress [1]. The partial differential equations (PDEs) of heat conduction represent the mathematical model of the heat conduction phenomena of physical problems defined in the solid domain. Therefore, it serves as a fundamental tool in analyzing such problems and, in turn, offers an insight into how heat propagates over time and spatial direction. However, the analytic solution of the PDEs is possible for the simple problems [2], and/or it requires a quite difficult solution process with different methods [3-5]. In many real problems, solving the PDEs analytically can be challenging due to complex geometries, the number of dependent variables, boundary conditions, etc. In this regard, numerical approaches employing finite difference (FDM) [6], finite element (FEM) [7], and finite volume methods (FVM) [8] offer the approximate solution of the PDEs.

The three methods aim to discretize and solve the PDEs but the discretization methods differ from each other

*Corresponding author:
Email: melih.yildiz@igdir.edu.tr

Cite this article as:
Yıldız, M. (2024). Solution scheme development of the nonhomogeneous heat conduction equation in cylindrical coordinates with neumann boundary condition by finite difference method. *European Mechanical Science*, *8*(3): 179-190. https://doi.org/10.26701/ems.1469706

History dates:
Received: 17.04.2024, *Revision Request*: 01.07.2024, *Last Revision Received*: 11.07.2024, *Accepted*: 23.07.2024

in these methods. The FDM approximates the PDEs by using a local Taylor expansion while the integral forms of the PDEs are used in the FEM and the FVM. Besides, the FDM uses generally a square grid structure to discretize the PDEs while the FEM and FVM offer to discretize the PDEs defined in more complex geometries [9]. Therefore, the FDM is frequently applied to issues involving regular geometry and is rather easy to apply. There are two main strategies used in numerical methods for solving PDEs: explicit and implicit schemes. The explicit approach updates the unknown function at each grid point by considering known values at each time step and/or grid point, which results in simple algebraic equations. Alternatively, the implicit method uses the values of the unknown function at each grid point for both the current and prior time steps and/or grid points. Thus, the implicit method is computationally more expensive than explicit methods. However, the implicit method offers typically unconditionally stable solutions while the explicit method has a stability restriction. Fine grid structures are needed to overcome the stability issue in the explicit technique, which raises computational costs for particularly stiff problems. In addition to two methods, the Crank-Nicolson method, known as implicit method [10], averages the explicit and implicit methods. As the Crank-Nicolson approach is second-order accurate in time, the solution is more accurate and stable [11].

In many research, the FDM was used for solving the partial differential heat conduction equations. Mojumder et al. [12] analyzed a one-dimensional transient heat conduction equation with Dirichlet boundary conditions in a cartesian coordinate system by using the explicit FDM and the Crank-Nicolson method. They reported that the Crank Nicolson method is unconditionally stable while the explicit scheme is only stable in a certain range of the Courant-Friedrichs-Lewy (CFL) condition criteria. Similarly, using both the explicit and implicit FDM method, Suarez-Carreno and Rosales-Romero [13] examined the one-dimensional transient heat conduction equation with Dirichlet boundary conditions in a cartesian coordinate system. They stated that the accuracy of the methods relies on the time step and grid size, and that the Crank-Nicolson technique is unconditionally stable. Whole et al.[14] implemented the explicit finite difference method for a two-dimensional steady-state heat conduction problem with Dirichlet boundary conditions in cartesian coordinates. They presented that the solutions obtained from the finite difference method have low errors comparing to the analytical solutions. Rieth et al.[15] presented the implicit FDM schemes for the generalized heat conduction equation in one spatial dimension for a shifted field approach. They compared the results with those obtained by the finite element method. They reported that the Crank-Nicolson type implicit scheme resulted in the most accurate. Han and Dai [16] presented the finite difference schemes by combining the Crank-Nicolson method and Richardson extrapolation which are unconditionally stable and provide better accurate solutions for the heat conduction equation with Neumann and Dirichlet boundary conditions in a one-dimensional domain. In the same manner, Yosaf et al.[17] carried out the solving of one-dimensional heat equations with Dirichlet and Neumann boundary conditions by developing a higher-order compact finite difference method. Dai [18] presented an extensive study on the heat conduction equation with Neumann boundary conditions for cartesian, cylindrical, and spherical coordinates by the finite difference schemes combining Crank-Nicolson or higher-order methods. They reported that the developed schemes are unconditionally stable and have high-fidelity solutions.

The literature survey shows that most of the studies using the FDM methods have focused on solving the homogeneous partial differential heat conduction equation, meaning without source term. Besides, the schemes in these studies have been presented mostly in cartesian coordinates. The current study aimed to develop finite difference schemes for the heat conduction problem including highly varying heat generating in cylindrical solid domains like batteries, nuclear fuel rods, etc. Therefore, the explicit finite difference and the Crank-Nicolson finite difference schemes were developed for the non-homogeneous partial differential heat conduction equation with the Neumann boundary conditions. The non-homogenous partial differential equation was also solved by the Matlab built-in function pdepe solver used in many studies [19- 21] to validate the developed schemes with a test problem defined by the determination of temperature distribution through a battery discharge period. Thus, the relative errors of the developed schemes were determined by comparing the results with those obtained from the pdepe solver. Besides, the stability criteria of these schemes were evaluated testing CFL conditions.

2. Model Equations and Finite Difference Scheme Development

Considering the one-dimensional heat conduction in the cylindrical coordinates with initial and Neumann boundary conditions which are axial symmetric boundary at r=0 and the convection heat transfer at r=R in an ambient temperature of T_∞, the governing partial differential heat conduction equation is as follows;

$$\frac{1}{r}\frac{\partial}{\partial r}\left(r\frac{\partial T}{\partial r}\right)+\frac{1}{k}s(r,t)=\frac{1}{\alpha}\frac{\partial T}{\partial t}$$
$$0<r\leq R, 0<t\leq t_s\,, \qquad (1.a)$$

or,

$$\frac{\partial^2 T}{\partial r^2}+\frac{1}{r}\frac{\partial T}{\partial r}+\frac{1}{k}s(r,t)=\frac{1}{\alpha}\frac{\partial T}{\partial t}$$
$$0<r\le R, 0<t\le t_s\,, \quad (1.b)$$

where, k and α are the thermal conductivity and thermal diffusivity, respectively. s denotes the heat generation or source term.

When examining Equation 1b, it has an indeterminate form 0/0 ratio at r =0 due to the second term (1/r ΔT/Δr). By employing L'Hospital's rule as in Equation 2, Equation 1.b at r =0 becomes Equation 3.

$$\left(\frac{1}{r}\frac{\partial T}{\partial r}\right)_{r=0}=\frac{(\frac{\partial}{\partial r})(\frac{\partial T}{\partial r})}{(\frac{\partial}{\partial r})(r)}=\left.\frac{\partial^2 T}{\partial r^2}\right|_{r=0} \quad (2)$$

$$2\frac{\partial^2 T}{\partial r^2}+\frac{1}{k}s(r,t)=\frac{1}{\alpha}\frac{\partial T}{\partial t} \qquad r=0, 0<t\le t_s\,, \quad (3)$$

The initial and boundary conditions are given below.

$$T(r,0)=T_\infty, \qquad r\in[0,R], \quad (4)$$

$$\frac{\partial T(0,t)}{\partial r}=0, \qquad t\in[0,t_s] \quad (5.a)$$

$$\frac{\partial T(R,t)}{\partial r}=-\frac{h}{k}[T(R,t)-T_\infty], \qquad t\in[0,t_s] \quad (5.b)$$

Equation 5.a is due to the axial symmetric boundary at r=0, and Equation 5.b implies the convective heat transfer at r=R.

It is now examined the numerical solution schemes development, based on the finite difference method-Explicit method and the Crank Nicolson Implicit method. Let *m* and *k* be the number of nodes on a grid structure for the spatial and time variables, respectively. Thus, the grid steps and the grid structure, Ω as shown in ▶**Figure 1**, are defined as follows.

$$\Delta r=\frac{R}{m}, \quad \Delta t=\frac{t_s}{k} \quad (6.a)$$

and,

$$\Omega=\{(r_i,t_\tau): r_i=i\Delta r, t_\tau=\tau\Delta t, i=0,1,\dots,m, \tau=0,1,\dots,k\} \quad (6.b)$$

2.1. Explicit Method

The governing equations require approximations for the first and second derivate in space, and the first derivate in time. By using the first-order forward finite-difference and the second-order centered finite-divided differences formula, the first and second derivate terms are discretized as follows.

The second order centered finite- difference formula:

$$\frac{\partial^2 T}{\partial r^2}\cong\frac{T_{i+1}^{\tau}-2T_i^{\tau}+T_{i-1}^{\tau}}{(\Delta r)^2} \quad (7)$$

The firs order forward finite- difference formula:

$$\frac{\partial T}{\partial r}\cong\frac{T_{i+1}^{\tau}-T_i^{\tau}}{\Delta r} \quad (8.a)$$

and,

$$\frac{\partial T}{\partial t}\cong\frac{T_i^{\tau+1}-T_i^{\tau}}{\Delta t} \quad (8.b)$$

By substituting Eq.7, and Eq.8.a,b into Eq.1.b and Eq.3, the resulting explicit finite-difference approximations become as below.

For Eq.1.b:

$$\frac{T_{i+1}^{\tau}-2T_i^{\tau}+T_{i-1}^{\tau}}{(\Delta r)^2}+\frac{1}{i.\Delta r}\frac{T_{i+1}^{\tau}-T_i^{\tau}}{\Delta r}+\frac{1}{k}s_i^t=\frac{1}{\alpha}\frac{T_i^{\tau+1}-T_i^{\tau}}{\Delta t} \quad for\ i>0\ (r\neq 0) \quad (9)$$

For Eq.3:

$$2\frac{T_{i+1}^{\tau}-2T_i^{\tau}+T_{i-1}^{\tau}}{(\Delta r)^2}++\frac{1}{k}s_i^t=\frac{1}{\alpha}\frac{T_i^{\tau+1}-T_i^{\tau}}{\Delta t} \quad for\ i=0 \quad (r=0) \quad (10)$$

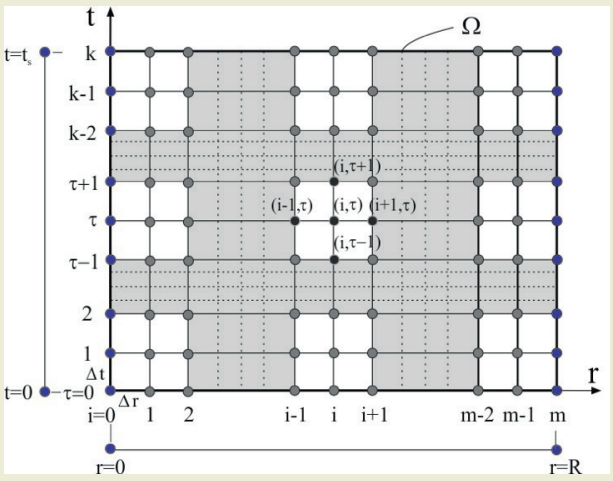

Figure 1. The schematic grid structure for the finite difference discretization

By arranging Eq.9 and Eq.10,

$$T_i^{\tau+1} = KT_{i-1}^{\tau} + \left[1 - K\left(2 + \frac{1}{i}\right)\right] T_i^{\tau} + K\left(1 + \frac{1}{i}\right) T_{i+1}^{\tau} + \alpha \Delta t G_i^{\tau}, \quad for\ 0 < i < m\ \ (r \neq 0) \tag{11}$$

and,

$$T_i^{\tau+1} = 2KT_{i-1}^{\tau} + (1 - 4K)T_i^{\tau} + 2KT_{i+1}^{\tau} + \alpha \Delta t G_i^{\tau}\ ,\ \ for\ \ i = 0\ \ (\ r = 0) \tag{12}$$

where,

$$K = \frac{\alpha \Delta t}{(\Delta r)^2}\ ,and\ \ G_i^{\tau} = \frac{1}{k}\, s_i^{\tau} \tag{13}$$

Additionally, the nodes *i-1* and *i+1* are fictitious nodes meaning a fictitious temperature for the defining nodes corresponding to *r=0* and *r=R*. Therefore, by applying a second-order central difference formula to the boundary conditions, the fictitious temperatures are eliminated as follows.

$$\left.\frac{T_{i+1}^{\tau} - T_{i-1}^{\tau}}{2\Delta r}\right|_{r=0} = 0, \quad giving;\ \ T_{i+1}^{\tau} = T_{i-1}^{\tau} \tag{14}$$

$$\left.\frac{T_{i+1}^{\tau} - T_{i-1}^{\tau}}{2\Delta r}\right|_{r=R} = -\frac{h}{k}\,(T_i^{\tau} - T_{\infty}),$$

$$giving;\ \ T_{i+1}^{\tau} = T_{i-1}^{\tau} - \frac{2\Delta r h}{k} T_i^{\tau} + \frac{2\Delta r h}{k} T_{\infty} \tag{15}$$

By introducing Eq.14 into 12, and Eq.15 into 11, the finite difference equations for boundary nodes are obtained as

$$T_i^{\tau+1} = (1 - 4K)T_i^{\tau} + 4KT_{i+1}^{\tau} + \alpha \Delta t G_i^{\tau}\ ,\ \ for\ \ i = 0\ \ (r = 0) \tag{16}$$

and,

$$T_i^{\tau+1} = K(2 + \frac{1}{i})T_{i-1}^{\tau} + \left[1 - K\left(2 + \frac{1}{i}\right) - KH\left(1 + \frac{1}{i}\right)\right] T_i^{\tau} + KH\left(1 + \frac{1}{i}\right) T_{\infty} + \alpha \Delta t G_i^{\tau}\ \ for\ \ i = m\ (r = R) \tag{17}$$

where, H=2Δrh/k.

Ultimately, the governing equation defined by Eq.1a or 1b with the initial and boundary conditions is solved by the obtained explicit finite difference approximations which are Eq.16 (for boundary node at *r = 0*), Eq.11 (for interior nodes), and Eq.17 (for boundary node at *r =R*). The numerical scheme provides an equation system including *m* algebraic equations for τ number with Δ*t* interval. The equation system is given in the matrix form as follows.

$$\begin{Bmatrix} T_0 \\ T_1 \\ T_2 \\ . \\ . \\ . \\ T_{m-1} \\ T_m \end{Bmatrix}^{\tau+1} = \begin{bmatrix} 1-4K & 4K & \square & \square & \square & \square & \square \\ K & \beta_{1,i} & \beta_{2,i} & \square & \square & \square & \square \\ \square & K & \beta_{1,i} & \beta_{2,i} & \square & \square & \square \\ \square & \square & . & . & . & \square & \square \\ \square & \square & \square & . & . & . & \square \\ \square & \square & \square & \square & K & \beta_{1,i} & \beta_{2,i} \\ \square & \square & \square & \square & \square & \beta_{3,i} & \beta_{4,i} \end{bmatrix} \begin{Bmatrix} T_0 \\ T_1 \\ T_2 \\ . \\ . \\ . \\ T_{m-1} \\ T_m \end{Bmatrix}^{\tau} + \begin{Bmatrix} \alpha \Delta t G_0 \\ \alpha \Delta t G_1 \\ \alpha \Delta t G_2 \\ . \\ . \\ . \\ \alpha \Delta t G_{m-1} \\ \alpha \Delta t G_m + KH(1 + \frac{1}{m}) \end{Bmatrix}^{\tau} \tag{18}$$

where,

$$\beta_{1,i} = 1 - K\left(2 + \frac{1}{i}\right), \beta_{2,i} = K\left(1 + \frac{1}{i}\right),\ \ \beta_{3,i} = K\left(2 + \frac{1}{i}\right),\ \ \beta_{4,i} = 1 - K\left(2 + \frac{1}{i}\right) - KH\left(1 + \frac{1}{i}\right)$$

Thus, Eq.18 is solved up to a given time by starting the initial condition values.

2.2. The Crank Nicolson Method

The explicit finite difference approximations can result in a problem with stability. To overcome the problem, the implicit finite-difference methods are an alternative way that is somewhat more complicated than the explicit method. The simple implicit method is unconditionally

stable but limits the use of large-time steps for reasonable accuracy [10]. In this regard, the Crank-Nicolson method presents an implicit scheme that is second-order accurate in both spatial and time. Therefore, it gives a high level of accuracy with a coarser grid in the time. In the current study, the first and second derivate terms were discretized by the Crank-Nicolson method as follows.

$$\frac{\partial^2 T}{\partial r^2} \cong \frac{1}{2}\left[\frac{T_{i+1}^{\tau} - 2T_i^{\tau} + T_{i-1}^{\tau}}{(\Delta r)^2} + \frac{T_{i+1}^{\tau+1} - 2T_i^{\tau+1} + T_{i-1}^{\tau+1}}{(\Delta r)^2}\right] \tag{19}$$

$$\frac{\partial T}{\partial r} \cong \frac{1}{2}\left[\frac{T_{i+1}^{\tau} - T_i^{\tau}}{\Delta r} + \frac{T_{i+1}^{\tau+1} - T_i^{\tau+1}}{\Delta r}\right] \tag{20}$$

$$\frac{\partial T}{\partial t} \cong \frac{T_i^{\tau+1} - T_i^{\tau}}{\Delta t} \tag{21}$$

,and

$$G_i^{\tau+1/2} = \frac{G_i^{\tau+1} + G_i^{\tau}}{2} \tag{22}$$

By substituting Eq.19, Eq.20, Eq.21, and Eq.22 into Eq.1.b and Eq.3, the resulting Crank-Nicolson approximations become as below.

$$\begin{aligned} &-\theta T_{i-1}^{\tau+1} + \left[1 + \theta\left(\frac{1}{i} + 2\right)\right] T_i^{\tau+1} - \theta\left(1 + \frac{1}{i}\right) T_{i+1}^{\tau+1} \\ &= \theta T_{i-1}^{\tau} + \left[1 - \theta\left(\frac{1}{i} + 2\right)\right] T_i^{\tau} + \theta\left(1 + \frac{1}{i}\right) T_{i+1}^{\tau} \\ &\quad + \alpha \Delta t G_i^{\tau+1/2} \\ &\quad for\ 0 < i < m\ (r \neq 0) \end{aligned} \tag{23}$$

,and

$$\begin{aligned} &K T_{i-1}^{\tau} + (1 - 2K) T_i^{\tau} + K T_{i+1}^{\tau} + \alpha \Delta t G_i^{\tau} \\ &\quad = -K T_{i-1}^{\tau+1} + (1 + 2K) T_i^{\tau+1} - K T_{i+1}^{\tau+1} \\ &\quad for\ \ i = 0\ \ (\ r = 0) \end{aligned} \tag{24}$$

where, $\theta = K/2 = \alpha \Delta t\ /\ 2(\Delta r)^2$.

By applying boundary conditions to Eq. 23 for the node at $r=R$ (for $i=m$), and to Eq.24 for the node at $r=0$ (for $i=0$), the following finite-difference equations are obtained.

$$\begin{aligned} &-\theta(2 + \frac{1}{i}) T_{i-1}^{\tau+1} + \left[1 + \theta(\frac{1}{i} + H\left(1 + \frac{1}{i}\right) + 2)\right] T_i^{\tau+1} \\ &\quad = \theta(2 + \frac{1}{i}) T_{i-1}^{\tau} + \left[1 - \theta(\frac{1}{i} + H\left(1 + \frac{1}{i}\right) + 2)\right] T_i^{\tau} \\ &\quad + 2\theta H\left(1 + \frac{1}{i}\right) T_{\infty} + \alpha \Delta t G_i^{\tau+1/2} \quad for\ i = m \end{aligned} \tag{25}$$

$$\begin{aligned} &(1 + 2K) T_i^{\tau+1} - 2K T_{i+1}^{\tau+1} \\ &\quad = (1 - 2K) T_i^{\tau} + 2K T_{i+1}^{\tau} + \alpha \Delta t G_i^{\tau+\frac{1}{2}}, \\ &\quad for\ i = 0 \end{aligned} \tag{26}$$

Thus, by employing the finite difference equations, Eq. 23, 25, and 26, the equation system in the matrix form is written as,

$$\begin{bmatrix} 1+2K & -2K & \square & \square & \square & \square & \square \\ -\theta & \lambda_{l1,i} & \lambda_{l2,i} & \square & \square & \square & \square \\ \square & -\theta & \lambda_{l1,i} & \lambda_{l2,i} & \square & \square & \square \\ \square & \square & . & . & . & \square & \square \\ \square & \square & \square & . & . & . & \square \\ \square & \square & \square & \square & -\theta & \lambda_{l1,i} & \lambda_{l2,i} \\ \square & \square & \square & \square & \square & \lambda_{l3,i} & \lambda_{l4,i} \end{bmatrix} \begin{Bmatrix} T_0 \\ T_1 \\ T_2 \\ . \\ . \\ . \\ T_{m-1} \\ T_m \end{Bmatrix}^{\tau+1} =$$

$$\begin{bmatrix} 1-2K & 2K & \square & \square & \square & \square & \square \\ \theta & \lambda_{r1,i} & -\lambda_{l2,i} & \square & \square & \square & \square \\ \square & \theta & \lambda_{r1,i} & -\lambda_{l2,i} & \square & \square & \square \\ \square & \square & . & . & . & \square & \square \\ \square & \square & \square & . & . & . & \square \\ \square & \square & \square & \square & \theta & \lambda_{r1,i} & -\lambda_{l2,i} \\ \square & \square & \square & \square & \square & -\lambda_{l3,i} & \lambda_{r4,i} \end{bmatrix} \begin{Bmatrix} T_0 \\ T_1 \\ T_2 \\ . \\ . \\ . \\ T_{m-1} \\ T_m \end{Bmatrix}^{\tau} + \begin{Bmatrix} \alpha \Delta t G_0 \\ \alpha \Delta t G_1 \\ \alpha \Delta t G_2 \\ . \\ . \\ . \\ \alpha \Delta t G_{m-1} \\ \alpha \Delta t G_m + 2\theta H\left(1 + \frac{1}{m}\right) T_{\infty} \end{Bmatrix}^{\tau+1/2} \tag{27}$$

where,

$$\lambda_{l1,i} = 1 + \theta\left(2 + \frac{1}{i}\right), \quad \lambda_{r1,i} = 1 - \theta\left(2 + \frac{1}{i}\right)$$

$$\lambda_{l2,i} = -\theta\left(1 + \frac{1}{i}\right), \quad \lambda_{l3,i} = -\theta\left(2 + \frac{1}{i}\right),$$

$$\lambda_{l4,i} = 1 + \theta\left(\frac{1}{i} + H\left(1 + \frac{1}{i}\right) + 2\right),$$

$$\lambda_{r4,i} = 1 - \theta(\frac{1}{i} + H\left(1 + \frac{1}{i}\right) + 2)$$

By defining the coefficient matrixes and the vectors in

the right and left side hand of Eq.27 as [L], [R], {T}, and {Nh}, the equation can be written as follows.

$$[L]\{T\}^{\tau+1} = [R]\{T\}^{\tau} + \{Nh\}^{\tau+1/2} \tag{28}$$

By multiplying both sides of the equation by the inverse of matrix L, Eq.28 becomes in the form as follows,

$$\{T\}^{\tau+1} = [L]^{-1}[R]\{T\}^{\tau} + [L]^{-1}\{Nh\}^{\tau+1/2} \tag{29}$$

As in the explicit method, Eq.29 is solved by starting with initial values for a given time.

3. The pdepe Solver Model

The model equation was also solved using the Matlab built-in function *pdepe* which solves initial-boundary elliptic and parabolic partial differential equation (PDEs), systems in one spatial variable and time. In the pdepe solver, the approximate solution is obtained by integrating the ordinary differential equations (ODEs) in a certain time, emerging with spatial discretization [22].

The general form of the equation in *pdepe* solver is defined as follows [23].

$$c\left(x,t,u,\frac{\partial u}{\partial x}\right)\frac{\partial u}{\partial t} = x^{-m}\frac{\partial}{\partial x}\left(x^{m} f\left(x,t,u,\frac{\partial u}{\partial x}\right)\right) + s\left(x,t,u,\frac{\partial u}{\partial t}\right) \tag{30}$$

When considering the general form for m=1, it resembles Equation 1. a. The variables, u, x correspond to T and r in Equation 1.a. Thus, the functions *c, f,* and *s* are defined as

$$c = \frac{1}{\alpha}, \qquad f = \frac{\partial u}{\partial x}, \text{and} \qquad s = G(x,t) \tag{31}$$

To implement the *pdepe* solver, the initial and boundary conditions are defined in sub-functions with the form as follows.

Initial condition:

$$u(x,0) = u0 = T_{\infty} \tag{32}$$

The *pdepe* solver satisfies the boundary conditions as following equation form.

$$p(x,t,u) + q(x,t) f\left(x,t,u,\frac{\partial u}{\partial x}\right) = 0 \tag{33}$$

Recalling boundary conditions given in Eq.5.a ,b, the p and q were defined as follows.

$$\begin{aligned} pl &= 0, & ql &= 1, \ left\ side\ (at\ r = 0) \\ pr &= \frac{h}{k}.(ur - T_{\infty}), & qr &= 1, right\ side\ (at\ r = R) \end{aligned} \tag{34}$$

4. Implementation

The developed numerical schemes were applied to a physical model of a cylindrical battery cell to determine time-dependent temperature variation in the radial direction of the cell. The geometric and thermophysical properties are given in ▶Table 1. To define the heat source during the discharge period of the cell, the volumetric heat generation was regarded as a time-dependent polynomial function derived from the study performed by Hwang et al.[24]. The equation was obtained at 1C discharging rate meaning that the total simulation time is 3600 s.

$$\begin{aligned} s(t) &= 59116.31 + 58.03t - 0.138t^2 \\ &+ 1.102\ 10^{-4}t^3 - 3.75110^{-8}t^4 \\ &+ 4.683\ 10^{-12}t^5 \end{aligned} \tag{35}$$

The function values defined by G in Eq.13 and Eq.31 were, thus, attained by dividing the k value.

To implement the developed solving schemes and the *pdepe* solver for the problem, it was assumed that the initial temperature, T_0 is equal to T_{∞} which is the ambient temperature of 25 °C. Furthermore, the convective heat transfer coefficient between the battery surface and the ambient is regarded as 10 W/m²K [25].

Table 1. The battery cell specifications [24, 26]

Properties	Value
Radius	9 mm
Density(ρ)	2939 kg/m³
Conductivity (k)	1.6 W/mK
Specific heat (cp)	2400 j/kg.K
Thermal diffusivity (m²/s)	2.268 10^{-7} m²/s

The developed numerical schemes were coded in Matlab and tested with the model defined above. The CFL condition was first investigated for a stable solution of the explicit method. The results were compared in stable conditions with those obtained by the pdepe solver known as the unconditionally stable and high accuracy numerical approach. Moreover, the computational per-

formances of three solution schemes were evaluated in the same grid structures in terms of CPU time.

5. Results

In this section, the stability of the developed schemes, and the results of the numerical schemes implemented for the battery problem in stable condition are presented by comparing them to those obtained from the pdepe solver.

5.1. Stability Evaluation of the Developed Numerical Schemes

Stability in numerical schemes is crucial for obtaining accurate and reliable solutions to mathematical problems. A stable numerical scheme enables accurate and reliable results over time. Otherwise, the numerical scheme amplifies errors or produces wildly fluctuating solutions in unstable conditions. Many techniques have been developed for stability analysis such as von Neumann stability analysis [27], and Courant–Friedrichs–Lewy (CFL) condition [28]. The CFL condition for the numerical schemes of a typical one-dimensional heat conduction equation states that the time step and thermal diffusivity divided by the square of the spatial step size must be less than a certain value for stability [10]. Therefore, the K value given in Eq.13 becomes the criteria for stability investigation.

Figure 2 shows the instability of the explicit scheme for two K values obtained by changing the time step (Δt). As seen in ▶**Figure 1a**, the instability at K=0.3714 with Δt=1.64 has a maximum amplitude of fluctuation with an order of 10^{35} and it grows early time stage of the total simulation period. ▶**Figure 1b** illustrates that the instability partially alleviates due to decreasing the K value, as the stability both grows later time stage and has lower maximum fluctuation than those of K=0.3714.

To reveal the effect of Δr and Δt together on the instability of the explicit scheme, the solution of the explicit scheme with Δr = 1.1e-3 and Δt=2.06 was tested. Thus, the K value was kept at 0.3689 around the values of the cases in ▶**Figure 2**. As seen in ▶**Figure 3**, although the time step increases the instability of the solution doesn't result in higher order fluctuation than the case in ▶**Figure 2a** due to increasing also the spatial step size.

To determine the CFL condition for the stability of the developed explicit scheme, several trials were tested, ultimately, the stable solution of the explicit scheme was provided in the case of K ≤0.3404 as shown in ▶**Figure 4**. Besides, although the solution at K=0.3599 resembles a stable solution it is an inconsistent solution due to the constant temperature values for each a certain time interval.

The thermal diffusivity α also influences the stability. ▶**Figure 5** shows the thermal diffusivity effect on the stability. If α becomes 2.55 e-7 m^2/s instead of 2.27e-7 m^2/s, the explicit numerical scheme results in an unstable solution due to increasing K value as seen in ▶**Figure 5**. The solution illustrated in ▶**Figure 5** proves the CFL condition depends on the *K* value. Consequently, if the CFL condition is not satisfied, an unstable numerical solution leads to non-physical phenomena like oscillations or divergent solutions. The stability criterion of the developed explicit scheme is determined as $0 < K \leq 0.3404$.

Figure 7 verifies the finite difference scheme based on the Crank-Nicolson method to be unconditionally stable as stated in the study [29]. As can be seen in ▶**Figure 6** for three different K values by changing the time step, the Crank Nicolson scheme gives stable solutions

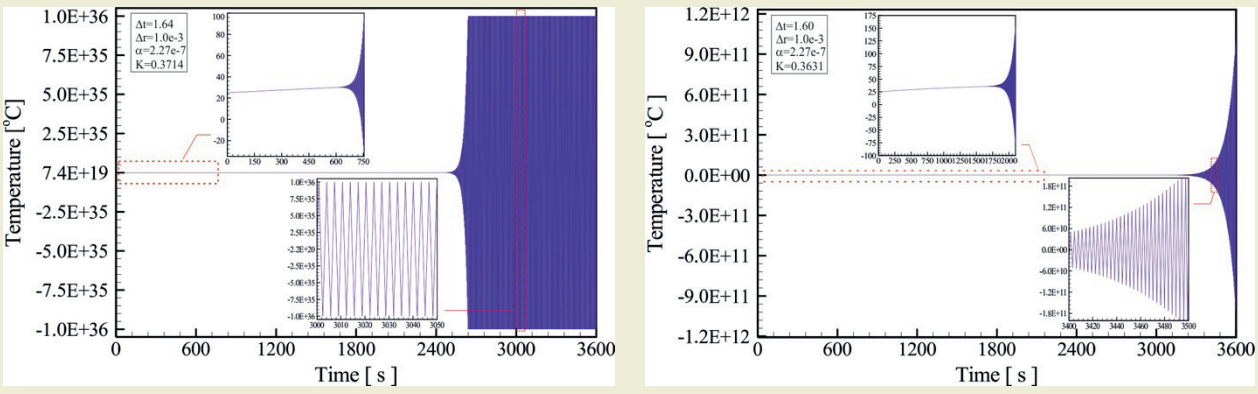

(a) (b)

Figure 2. Unstable solution in explicit scheme at spatial domain r= 9 mm **(a)** *K*=0.3714, **(b)** *K*= 0.3631

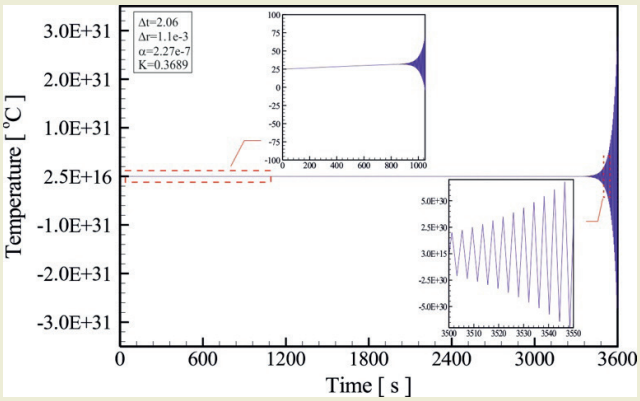

Figure 3. Unstable solution in the explicit scheme for □r=1.1e-3 m and □t=2.06 s at r=9 mm

Table 2. The temperature values obtained from the Crank-Nicolson scheme at t=3600 s for different K values by changing time steps

Time step [s]	Δt=1.0 (K=0.2269)	Δt=4.5 (K=1.0022)	Δt=225 (K=51.0380)
Temperature [°C]	45.9574	45.9575	46.0850

in each case even if the K value is quite greater than the stability criterion of 0.3404 of the explicit scheme. Unsurprisingly, the change in the time step influences the results. It should be also noted that smaller time step allows the more accurate results due to definition of derivate [30]. ▶**Table 2** presents the temperature values at 3600 s and r=9 mm for the Crank Nicolson scheme. The differences in the temperature values relative to Δt=1.0 s are 0.0001 °C and 0.1276 °C for Δt= 4.5 s and 225 s, respectively.

5.2. Comparison of the Numerical Solutions:

The finite difference schemes' results were compared to those obtained from the pdepe solver with the same grid structures in stable conditions. ▶**Figure 7** shows the time-dependent temperature variations at r=9 mm obtained from the numerical methods with the two grid structures. As seen in the Figure, the results of the two schemes developed are nearly identical. Moreover, the results of the schemes approach those of the pdepe solver when the grid structure gets fine size. ▶**Figure 8** also illustrates the absolute error of both the schemes developed relative to the results of the pdepe solver. The absolute error changes in time due to including highly

Table 3. Comparison of temperature values at different radial positions and times (Δr=0.5e-3 m, Δt=0.25 s)

	Temperature [°C]									
	ES	CN	pdepe	$\|\Delta T_{ES}\|$	$\|\Delta T_{CN}\|$	ES	CN	pdepe	$\|\Delta T_{ES}\|$	$\|\Delta T_{CN}\|$
Time [s]			r=4 mm					r=8 mm		
900	32.1442	32.1439	32.0865	0.0576	0.0574	32.0289	32.0287	31.9731	0.0558	0.0555
1800	36.5474	36.5470	36.5028	0.0446	0.0442	36.3589	36.3585	36.3165	0.0424	0.0420
3600	46.2708	46.2719	46.2761	0.0052	0.0042	45.9261	45.9272	45.9340	0.0078	0.0068

ES: Explicit scheme, CN: Crank Nicolson scheme
$|\Delta T_{ES}| = |T_{pdepe} - T_{ES}|$, $|\Delta T_{CN}| = |T_{pdepe} - T_{CN}|$

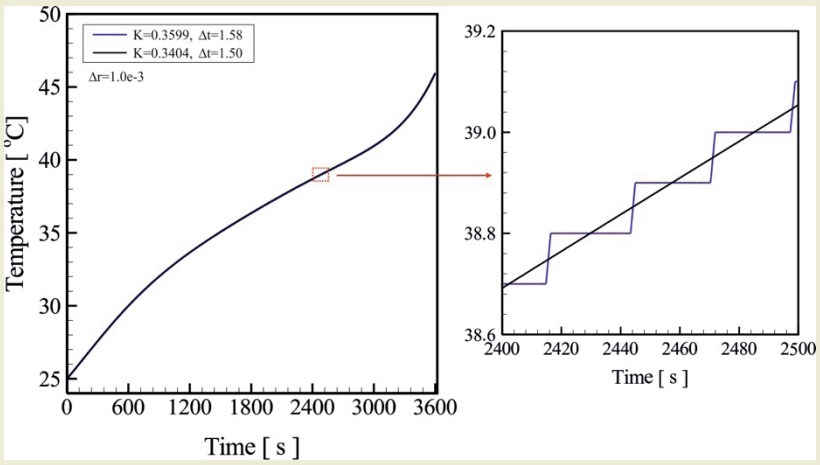

Figure 4. Stable and inconsistence solutions of the developed explicit scheme at r = 9 mm

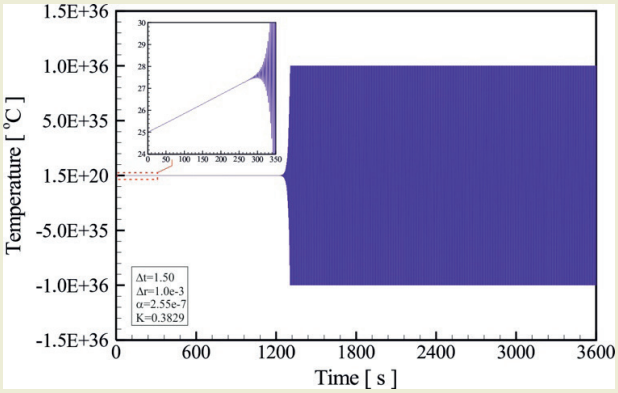

Figure 5. Unstable solution in the explicit scheme with α=2.55e-7

varying time-dependent heat generation terms as given in Eq.35. Thus, the maximum absolute error is about 0.2117 °C, corresponding to a maximum relative error of 0.43 %, at the grid structure with Δt=1.0 s and Δr=1.0e-3 m. In the grid structure of Δt=0.25 s and Δr=0.5e-3 m , it is about 0.0859 °C, corresponding to a maximum relative error of 0.21 %.

Figure 9 shows the results in the radial direction at different times, the difference temperature values between both the explicit and Crank Nicolson schemes are on the order of 10^{-4}. On the other hand, the temperature differences between the developed schemes and the pdepe solver change with time and are on the order of 10^{-2} and 10^{-3}. Similarly, ▶**Figure 10** illustrates these results given in ▶**Figure 9** in contour plots of the solutions of the defined time-dependent model equation in the radial direction. As shown in the plots in ▶**Figure 10**, the differences in temperature distributions are quietly low and they are nearly identical for three numerical solutions at t= 3600 s. Some numerical solutions and absolute errors, relative to the pdepe, are given in ▶**Table 3** for different times. The results suggest that the schemes developed are as reliable as the pdepe solver.

To evaluate the computational performance of the ex-

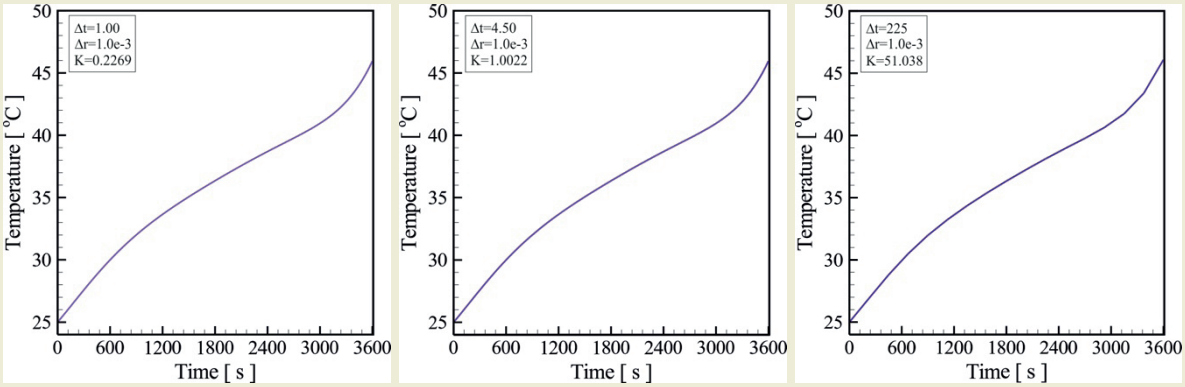

Figure 6. The Crank-Nicolson scheme solutions for different K values at r=9.0 mm

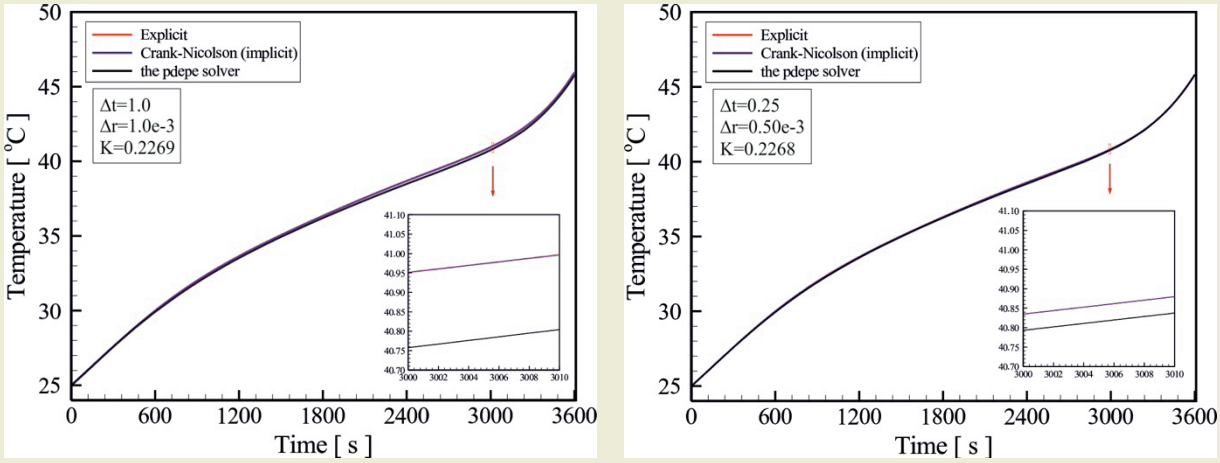

Figure 7. Comparison of the numerical solutions at r=9 mm

https://doi.org/10.26701/ems.1469706

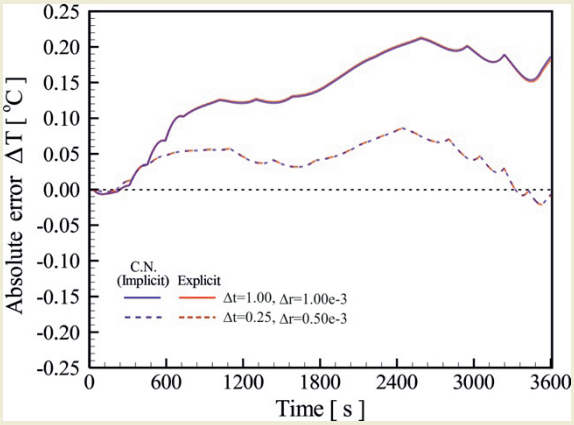

Figure 8. The absolute errors of the explicit and Crank-Nicolson schemes relative to the ***pdepe*** solver at r=9 mm

plicit and Crank-Nicolson FDM schemes in terms of computing time, the CPU times of the developed numerical schemes were compared to those of the pdepe solver in the same grid structures. All computational analyses were performed on a PC with a 2.00 GHz Intel (R) Core ™ i7-2630 CPU and 8 GB RAM. ▶**Table 3** presents the CPU times of the numerical schemes.

As shown in ▶**Table 4**, the developed explicit and Crank-Nicolson schemes consume fewer CPU times than those of the pdepe solver, as in the reference [31]. Besides, the explicit scheme has the least CPU times for

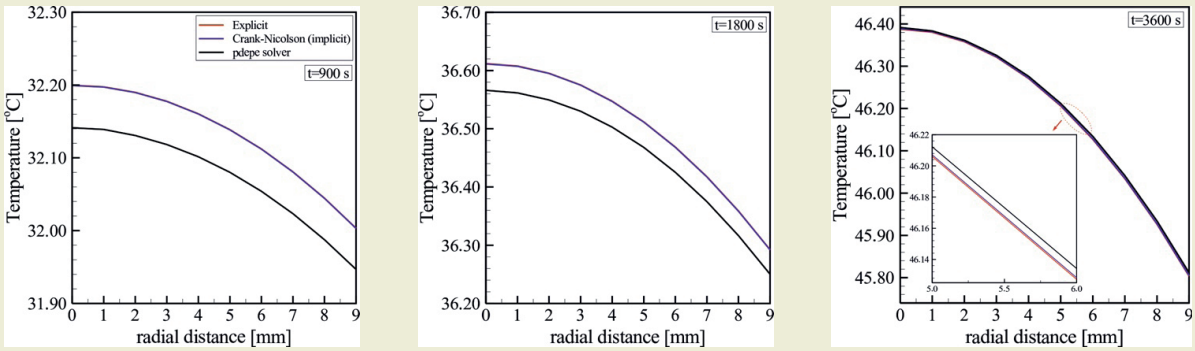

Figure 9. Comparison of the numerical solutions in radial direction at different times (Δr=0.5e-3 m, Δt=0.25 s)

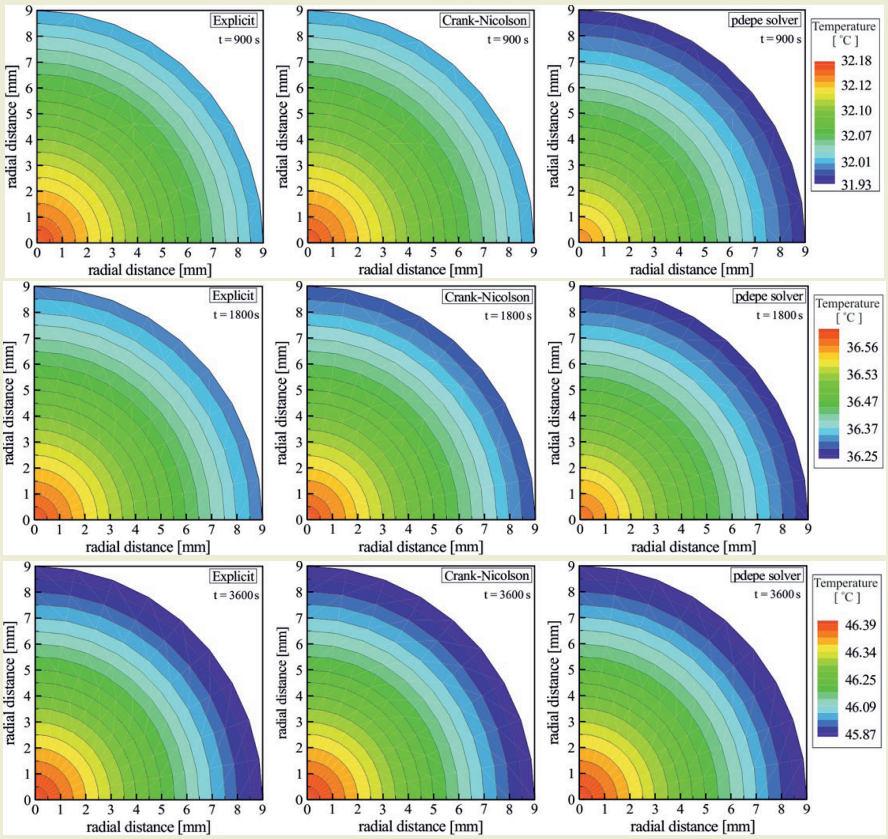

Figure 10. Temperature distribution, Δr=0.5e-3 m, Δt=0.25 s

Table 4. CPU time of the schemes developed and pdepe solver

	Grid structure	Explicit FDM	Crank-Nicolson FDM	Pdepe solver
CPU time [s]	Δr=1e-3, Δt=1.0	0.0342	0.0513	0.5133
	Δr=5e-4, Δt=0.25	0.0693	0.2015	0.8308
	Δr=2.65e-4, Δt=0.1	0.2064	0.9490	1.4283

each grid structure in stable conditions due to its solving scheme consisting of the simpler algebraic equation system.

6. Conclusions

In this research, the explicit and Crank-Nicolson FDM schemes were successfully developed for solving one-dimensional heat conduction equations including heat generation source terms with Neumann boundary conditions in cylindrical coordinates. The numerical schemes were, then, applied to solving the cylindrical battery problem including highly varying heat generation in time. The problem was also solved by the pdepe solver, a Matlab built-in function to verify the numerical schemes. Considering the results, the following main conclusion can be stated.

- The stability requirement for the developed explicit scheme was found to be the condition of $0 \leq K \leq 0.3404$. It is also shown that the developed Crank Nicolson FDM scheme is unconditionally stable with several trials of K values.
- The explicit and Crank Nicolson schemes give nearly identical results with the order of 10^{-4} differences. Comparing the developed schemes to the pdepe solver known as having high accuracy, the maximum relative errors to the pdepe solver results is about 0.21 % with the grid structure of Δt=0.25 s and Δr=0.5 mm.
- The developed schemes enable lower computational time than the pdepe solver when considering CPU time at the same grid structures.

As a general result, the developed schemes are as reliable as the pdepe solver. The numerical schemes can be applied to one-dimensional transient heat conduction problems with/without heat generation source terms, and Neumann boundary conditions in cylindrical coordinates.

Research Ethics

Ethical approval not required.

Author Contributions

The author(s) accept full responsibility for the content of this article and have approved its submission.

Competing Interests

The author(s) declare that there are no competing interests.

Research Funding

Not reported.

Data Availability

Not applicable.

Peer-review

Externally peer-reviewed.

7. References

[1] Çengel, Y. A. (2007). *Heat and mass transfer: A practical approach* (3rd ed.). McGraw-Hill Education.

[2] Götschel, S., & Weiser, M. (2019). Compression challenges in large scale partial differential equation solvers. *Algorithms, 12*(9), 197.

[3] Zada, L., Nawaz, R., Nisar, K. S., Tahir, M., Yavuz, M., Kaabar, M. K. A., & Martinez, F. (2021). New approximate-analytical solutions to partial differential equations via auxiliary function method. *Partial Differential Equations in Applied Mathematics, 4*, 100045.

[4] Chiang, K.-T., Kung, K.-Y., & Srivastava, H. M. (2009). Analytic transient solutions of a cylindrical heat equation with a heat source. *Applied Mathematics and Computation, 215*, 2877–2885.

[5] Cooper, J. (1998). Boundary value problems for heat equations. In *Introduction to partial differential equations with Matlab* (pp. 131–156). Birkhauser. https://doi.org/10.1007/978-1-4612-1754-1_4

[6] Hanafi, L., Mardlijah, M., Utomo, D. B., & Amiruddin, A. (2021). Study numerical scheme of finite difference for solution partial differential equation of parabolic type to heat conduction problem. *Journal of Physics: Conference Series, 1821*, 012032. https://doi.org/10.1088/1742-6596/1821/1/012032

[7] Taler, J., & Oclon, P. (2014). Finite element method in steady-state and transient heat conduction. In *Encyclopedia of thermal stresses* (pp. 1594–1600). Springer. https://doi.org/10.1007/978-94-007-2739-7_897

[8] Li, W., Yu, B., Wang, X., Wang, P., & Sun, S. (2012). A finite volume method for cylindrical heat conduction problems based on local analytical solution. *International Journal of Heat and Mass Transfer, 55*, 5570–5582.

[9] Peiro, J., & Sherwin, S. (2005). Finite difference, finite element and finite volume methods for partial differential equations. In *Handbook of materials modeling* (pp. 2417–2431). Springer. https://doi.org/10.1007/978-1-4020-3286-8_127

[10] Chapra, S. C., & Canale, R. P. (2015). *Numerical methods for engineers* (7th ed.). McGraw-Hill Education.

[11] Huang, P., Feng, X., & Liu, D. (2013). A stabilized finite element method for the time-dependent Stokes equations based on Crank-Nicolson scheme. *Applied Mathematical Modelling, 37,* 1910–1919.

[12] Mojumder, M., Haque, M., & Alam, M. (2023). Efficient finite difference methods for the numerical analysis of one-dimensional heat equation. *Journal of Applied Mathematics and Physics, 11,* 3099–3123. https://doi.org/10.4236/jamp.2023.1110204

[13] Suarez-Carreno, F., & Rosales-Romero, L. (2021). Convergency and stability of explicit and implicit schemes in the simulation of the heat equation. *Applied Sciences, 11,* 4468. https://doi.org/10.3390/app11104468

[14] Han, F., & Dai, W. (2013). New higher-order compact finite difference schemes for 1D heat conduction equations. *Applied Mathematical Modelling, 37,* 7940–7952.

[15] Whole, A., Lobo, M., & Ginting, K. B. (2021). The application of finite difference method on 2-D heat conductivity problem. *Journal of Physics: Conference Series, 2017,* 012009.

[16] Rieth, A., Kovacs, R., & Fülöp, T. (2018). Implicit numerical schemes for generalized heat conduction equation. *International Journal of Heat and Mass Transfer, 126,* 1177–1182.

[17] Yosaf, A., Rehman, S. U., Ahmad, F., Ullah, M. Z., & Alshomrani, A. S. (2016). Eighth-order compact finite difference scheme for 1D heat conduction equation. *Advances in Numerical Analysis,* 2016, Article ID 8376061, 12 pages. https://doi.org/10.1155/2016/8376061

[18] Dai, W. (2010). A new accurate finite difference scheme for Neumann (insulated) boundary condition of heat conduction. *International Journal of Thermal Science, 49,* 571–579.

[19] Kumar, D., Kumar, V., & Singh, V. P. (2010). Mathematical modeling of brown stock washing problems and their numerical solution using Matlab. *Computers & Chemical Engineering, 34,* 9–16.

[20] Li, Y.-X., Mishra, S. R., Pattnaik, P. K., Baag, S., Li, Y.-M., Khan, M. I., Khan, N. B., Alaoui, M. K., & Khan, S. U. (2022). Numerical treatment of time dependent magnetohydrodynamic nanofluid flow of mass and heat transport subject to chemical reaction and heat source. *Alexandria Engineering Journal, 61,* 2484–2491.

[21] Courtier, N. E., Richardson, G., & Foster, J. M. (2018). A fast and robust numerical scheme for solving models of charge carrier transport and ion vacancy motion in perovskite solar cells. *Applied Mathematical Modelling, 68,* 329–348.

[22] Yudianto, D., & Yuebo, X. (2010). A comparison of some numerical method in solving 1-D steady-state advection dispersion reaction equation. *Civil Engineering and Environmental Systems, 27*(2), 155–172.

[23] MathWorks. (n.d.). Partial differential equations. *MathWorks.* Retrieved February 8, 2024, from https://www.mathworks.com/help/matlab/math/partial-differential-equations.html

[24] Hwang, F. S., Confrey, T., Scully, S., Callaghan, D., Nolan, C., Kent, N., & Flannery, B. (2020). Modeling of heat generation in an 18650 lithium-ion battery cell under varying discharge rates. In *5th Thermal and Fluids Engineering Conference* (pp. 333–341). New Orleans, LA, USA.

[25] Wang, Z., Ma, J., & Zhang, L. (2017). Finite element thermal model and simulation for a cylindrical Li-ion battery. *IEEE Access, 5,* 15372–15379.

[26] Gümüşsu, E., Ekici, Ö., & Köksal, M. (2017). 3D CFD modeling and experimental testing of thermal behavior of Li-ion battery. *Applied Thermal Engineering, 120,* 484–495.

[27] Rostamy, D., & Abdollahi, N. (2019). Stability analysis for some numerical schemes of partial differential equation with extra measurements. *Hacettepe Journal of Mathematics & Statistics, 48*(5), 1324–1335.

[28] Trivellato, F., & Castelli, M. R. (2014). On the Courant-Friedrichs-Lewy criterion of rotating grids in 2D vertical-axis wind turbine analysis. *Renewable Energy, 62,* 53–62.

[29] Liu, W., & Wu, B. (2022). Unconditional stability and optimal error estimates of a Crank-Nicolson Legendre-Galerkin method for the two-dimensional second-order wave equation. *Numerical Algorithms, 90,* 137–158. https://doi.org/10.1007/s11075-021-01182-x

[30] Majchrzak, E., & Mochnacki, B. (2017). Implicit scheme of the finite difference method for 1D dual-phase lag equation. *Journal of Applied Mathematics and Computational Mechanics, 16*(3), 37–46.

[31] Khalifa, I. (2020). Comparing numerical methods for solving the Fisher equation (Master's thesis, Lappeenranta-Lahti University of Technology LUT, Finland).